tunable single-photon frequency converter in a waveguide with a giant V-type atom

Hongzheng Wu,¹ Ge Sun,^{1,2} Jing Lu,^{1,2} and Lan Zhou^{1,2,*}

¹Key Laboratory of Low-Dimension Quantum Structures and Quantum Control of Ministry of Education,
Key Laboratory for Matter Microstructure and Function of Hunan Province,
Synergetic Innovation Center for Quantum Effects and Applications,
Xiangjiang-Laboratory and Department of Physics,
Hunan Normal University, Changsha 410081, China
²Institute of Interdisciplinary Studies, Hunan Normal University, Changsha, 410081, China

We study the single-photon scattering in a one-dimensional (1D) waveguide coupled to one transition of a V-type giant atom (GA), whose other transition is coherently driven by an classical field. The inelastic scattering of single photons by the GA realizes the single-photon frequency conversion. By applying the Lippmann-Schwinger equation, the scattering coefficients for single photons incident from different directions are obtained, which present different scattering spectra in the Markovian and the non-Markovian regimes. The conversion contrast characterizing the nonreciprocity is also analyzed in both regimes. It is found that the probability of the frequency up- or down-conversion vanishes as long as the emission from either transition pathways for single photons is suppressed, but it is enhanced and even reach unity by introducing the nonreciprocity. It is the quantum self-interference induced by the scale of this two-legged GA and the phase difference between the GA-waveguide couplings that tune the probability of the frequency up- or down-conversion.

I. INTRODUCTION

Photons are ideal carriers of quantum information, as they interact only weakly with the environment, and their processes are fast and efficient. The practical absence of photon-photon interactions at the single-photon level in a vacuum makes it necessary to rely on the coupling of quantum emitters (QEs) and photons in order to attain nonlinearities at the level of individual photons, unfortunately, the strength of the single atom-photon interaction is intrinsically weak in free space. Nevertheless, the coupling can be substantially increased by placing the QEs in either high-finesse cavities[1, 2] or waveguides with strong-field confinement [3, 4]. In a one dimensional (1D) waveguide, the electromagnetic field is confined spatially in the transverse direction and maintain uniform in the longitudinal direction, which forms an effective one-dimensional (1D) continuum for propagating photons. The two ends of the waveguide are two natural ports for introducing and extracting information, and the photonic architecture of the waveguide coupled with QEs is convenient to design complex optical quantum devices, such as single-photon switches [5–9] and routers [10–19], diodes [20–22], et.al...

With the great technological progress of superconducting circuits, experiments on superconducting artificial QEs coupled to surface acoustic waves [23–25] or microwaves through multiple coupling points through suitably meandering the transmission line with wavelength-scale distance [26] have required going beyond the treatment of a QE as pointlike matter coupling locally to a waveguide. Such QEs in the literature are called "giant atoms (GAs)". Since the size of GAs is comparable to

or much larger than the wavelength of the electromagnetic radiation, the dipole approximation is no longer valid. The nonlocal GA-photon interaction leads to remarkable phenomena that are not present in quantum optics with pointlike QEs, such as frequency-dependent decay rate and collective Lamb shift [27–29] due to the self-interference induced by the scale of a GA, non-Markovian dynamics [30–33] and tunable atom-photon bound states [34–42] due to the significant internal time-delay for the field to propagate across the GA, waveguidemediated GA-GA interaction [43–48], nonreciprocal excitation transfer between GAs [49, 50] in an ordinary waveguide, etc..

To interface diverse quantum nodes that operate at different wavelengths in a quantum network, frequency conversion of photons are required. Although frequency conversion has been explored in the large photon flux limit, the capability of converting single photons from one frequency to another frequency is desired at the singlephoton level. Frequency converter have been proposed for single photons by a point-like three-level atom locally coupled to a Sagnac interferometer [51], a coupledresonator waveguide [52], a semi-infinite 1D transmission line [53]. Here, we propose a single-photon frequency converter based on the phases of the GA-waveguide coupling strengths. We notice that frequency conversions for a 1D waveguide with a GA have been proposed in Ref. [54, 55], however, the conversion efficiency in a convetional waveguide is at most one-half and the Markovian approximation is made in Ref [54], then two Sagnac interferometers are used to enhance the conversion efficiency. A conversion efficiency close to unity is found in Ref. [55], however chiral atom-waveguide couplings are necessary. In this paper, we exploit the self-interference induced by the scale of a two-legged GA to achieve singlephoton frequency conversion with efficiency close to unity in a conventional waveguide with linear light dispersion.

^{*} Corresponding author; zhoulan@hunnu.edu.cn

We apply the Lippmann-Schwinger equation for obtaining the scattering amplitudes when the travel time of the photon between adjacent coupling points is comparable to or larger than the inverse of the bare relaxation rate of the GA, then study the influence of the accumulated phases that photons travel between coupling points and the phase difference between the two coupling points on the scattering spectra and the conversion contrast in the Markovian and Non-Markovian regimes. The inelastic scattering of single photons by the GA enables the frequency conversion. The conversion probability in the system with reciprocity is at most one-half. To further improve the conversion probability, breaking the reciprocity is necessary. Thanks to the phase difference between GAwaveguide couplings which enables the nonreciprocal for photon scattering, the probability of the frequency upor down-conversion increases, and it even reached unity when atom-waveguide coupling are not chiral.

II. MODEL AND THE SCATTERING COEFFICIENTS

We consider a three-level giant atom (GA) with levels $|g\rangle,|f\rangle$, $|e\rangle$ form a V-type configuration, as shown in Fig.1. A classical driving field with frequency ω_d drives the transition $|f\rangle\leftrightarrow|e\rangle$ with the Rabi frequency Ω , and the transition $|g\rangle\leftrightarrow|e\rangle$ is coupled at positions $\pm d/2$ to a 1D waveguide with coupling strengths $J_j,j=1,2$, where couplings J_j are general complex. The 1D waveguide supports a continuum of electromagnetic modes, each associated with a wave vector k, frequency $\omega_k=v|k|$ and annihilation operators \hat{a}_k . The total Hamiltonian for this system reads

$$H = \omega_e |e\rangle\langle e| + (\omega_f - \omega_d)|f\rangle\langle f| + \int dk\omega_k \hat{a}_k^{\dagger} \hat{a}_k \qquad (1)$$
$$+\Omega|f\rangle\langle g| + \sum_{j=1}^2 \int dk J_j e^{(-1)^j ik \frac{d}{2}} \hat{a}_k^{\dagger} |g\rangle\langle e| + H.c.$$

The ground-state energy is set as the reference so that the energies of $|e\rangle$ and $|f\rangle$ are denoted by ω_f and ω_e , respectively. Ω is taken to be real. To write Eq.(1) in the rotating-wave approximation, it has been assumed that $\omega_f \simeq \omega_d$ and that frequencies ω_i , i = e, f, d are much larger than the coupling strengths J_i and Ω .

To find the GA's effect on a single photon incident from the waveguide, we introduce two dressed states

$$|\eta_{+}\rangle = \sin\frac{\theta}{2}|g\rangle + \cos\frac{\theta}{2}|f\rangle$$
 (2a)

$$|\eta_{-}\rangle = -\cos\frac{\theta}{2}|g\rangle + \sin\frac{\theta}{2}|f\rangle$$
 (2b)

with the corresponding eigenenergies

$$\nu_{\pm} = \frac{(\omega_f - \omega_d) \pm \sqrt{(\omega_f - \omega_d)^2 + 4|\Omega|^2}}{2}, \quad (3)$$

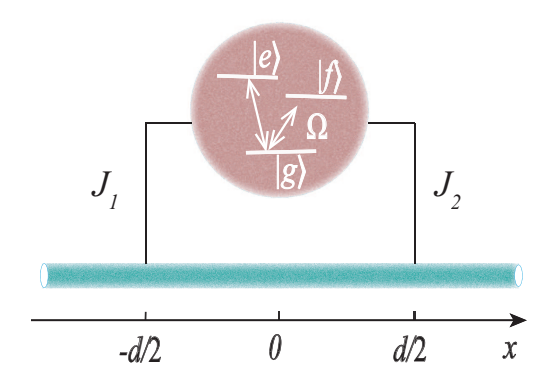


FIG. 1. Schematic of frequency conversion using a three-level GA with a V-type configuration coupled to a linear waveguide. The transition $|e\rangle\leftrightarrow|g\rangle$ is coupled to the waveguide at positions x=-d/2 and x=d/2, and transition $|g\rangle\leftrightarrow|f\rangle$ is driven by a classical field with frequency ω_d and Rabi frequency Ω .

and $\tan \theta = 2\Omega/(\omega_f - \omega_d)$. The Hamiltonian in Eq.(1) can be rewritten in terms of the dressed states as $H = H_0 + V$

$$H_{0} = \sum_{n=\pm} \nu_{n} |\eta_{n}\rangle \langle \eta_{n}| + \omega_{e} |e\rangle \langle e| + \int dk \omega_{k} \hat{a}_{k}^{\dagger} \hat{a}_{k} (4a)$$

$$V = \sum_{j=1}^{2} \int dk J_{js} e^{(-1)^{j} i k \frac{d}{2}} \hat{a}_{k}^{\dagger} |\eta_{+}\rangle \langle e| + H.c. \qquad (4b)$$

$$- \sum_{j=1}^{2} \int dk J_{jc} e^{(-1)^{j} i k \frac{d}{2}} \hat{a}_{k}^{\dagger} |\eta_{-}\rangle \langle e| - H.c.$$

with $J_{js} = J_j \sin \frac{\theta}{2}$ and $J_{jc} = J_j \cos \frac{\theta}{2}$. Here, H_0 is the free Hamiltonian for the 1D waveguide and the GA, V describes the GA-waveguide interaction. When an incoming photon with wavenumber k excites the GA from its initial state $|\eta_-\rangle$ ($|\eta_+\rangle$), the excited GA can spontaneously decay to either state $|\eta_-\rangle$ or $|\eta_+\rangle$ and emit a photon with frequency either unchanged or down-shifted (up-conversion). Consequently, the three-level atom acts as a frequency converter for single photons propagating in the 1D waveguide.

The total excitation number operator $\hat{N} = \int dk \hat{a}_k^{\dagger} \hat{a}_k + |e\rangle\langle e|$ commutes with the Hamiltonian H, states $\hat{a}_k^{\dagger} |0\eta_n\rangle, |0e\rangle$ are the eigenstates of the number operator \hat{N} in the subspace with one excitation, and they can expand the eigenstate $|\psi_{nk}^{+}\rangle$ of the Hamiltonian with a total energy $E_{nk} = v|k| + \nu_n$ as

$$\left|\psi_{nk}^{+}\right\rangle = \int dq \hat{a}_{q}^{\dagger} \left(\beta_{q} \left|0\eta_{+}\right\rangle + \chi_{q} \left|0\eta_{-}\right\rangle\right) + u_{kn} \left|0e\right\rangle, \quad (5)$$

where u_{kn} is the probability amplitude of the GA in the excited state while the field is in vacuum. β_q (χ_q) is the single-photon field amplitude while the GA is in the state

 $|\eta_{+}\rangle$ ($|\eta_{-}\rangle$). For photons propagating in a 1D waveguide and interacting with a GA scatterer, eigenstate $|\psi_{nk}^{+}\rangle$ also satisfies the Lippman-Schwinger equation [56]

$$\left|\psi_{nk}^{+}\right\rangle = \hat{a}_{k}^{\dagger}\left|0\eta_{n}\right\rangle + \frac{1}{E_{nk} - H_{0} + i\epsilon}V\left|\psi_{nk}^{+}\right\rangle. \tag{6}$$

Then, the probability amplitude of the GA's excitation reads

$$u_{kn} = \frac{\left(J_1^* e^{ik\frac{d}{2}} + J_2^* e^{-ik\frac{d}{2}}\right) \left(\delta_{n+} \sin\frac{\theta}{2} - \delta_{n-} \cos\frac{\theta}{2}\right)}{\Delta_k^n + i\Gamma + i\gamma \left(\sin^2\frac{\theta}{2} e^{-i\nu_+\tau} + \cos^2\frac{\theta}{2} e^{-i\nu_-\tau}\right) e^{iE_{nk}\tau}}$$
(7)

with $\tau = d/v$ the time taken by a photon to travel from one coupling point to the other coupling point, $\Delta_k^n = v|k| + \nu_n - \omega_e$ and

$$\Gamma = \frac{\pi}{v} (|J_1|^2 + |J_2|^2), \gamma = \frac{2\pi}{v} |J_1 J_2| \cos \varphi_J.$$
 (8)

Here, $\varphi_J = \varphi_1 - \varphi_2$ and φ_j is the phase of the coupling strength J_j . Note that $\Gamma = \Gamma_+ + \Gamma_-$ is also the radiative decay rates of a small atom, $\Gamma_+ = \Gamma \sin^2(\theta/2)$ and $\Gamma_- = \Gamma \cos^2(\theta/2)$ are the spontaneous decay rates of transitions $|e\rangle \leftrightarrow |\eta_+\rangle$ and $|e\rangle \leftrightarrow |\eta_-\rangle$ due to the coupling with the waveguide, respectively. In a similar way, the waveguidemediated nonlocal damping γ can be written as $\gamma = \gamma_+ + \gamma_-$ with $\gamma_+ = \gamma \sin^2(\theta/2)$ and $\gamma_- = \gamma \cos^2(\theta/2)$.

In the scattering theory formalism, the scattering matrix with element

$$S_{k'l;kn} = -2\pi i \delta \left(E_{k'l} - E_{kn} \right) \left(\delta_{l+} \sin \frac{\theta}{2} - \delta_{l-} \cos \frac{\theta}{2} \right) (9)$$
$$\times \left(J_1 e^{-ik'\frac{d}{2}} + J_2 e^{ik'\frac{d}{2}} \right) u_{kn} + \delta_{nl} \delta \left(k' - k \right).$$

connects states in the asymptotic past with states in the asymptotic future. The conservation of energy is showed in Eq.(9) via the delta Dirac function. For single photons incident from the negative channel with wave vector k > 0, the properties of the delta Dirac function give rise to the scattering amplitudes

$$t_{k-} = \frac{\Delta_{k}^{-} - \frac{2\pi}{v} J_{1c} J_{2c}^{*} \sin(\Delta_{k}^{-} \tau + \phi_{-}) + i\Gamma_{+} + i\gamma_{+} e^{i(\Delta_{k}^{-} \tau + \phi_{+})}}{\Delta_{k}^{-} + i\left(\Gamma_{+} + \gamma_{+} e^{i\phi_{+}} e^{i\Delta_{k}^{-} \tau}\right) + i\left(\Gamma_{-} + \gamma_{-} e^{i\phi_{-}} e^{i\Delta_{k}^{-} \tau}\right)} 10a)$$

$$r_{k-} = -\frac{i\gamma_{-} + \frac{\pi}{v} i \left[|J_{1c}|^{2} e^{i(\Delta_{k}^{-} \tau + \phi_{-})} + |J_{2c}|^{2} e^{-i(\Delta_{k}^{-} \tau + \phi_{-})} \right]}{\Delta_{k}^{-} + i\left(\Gamma_{+} + \gamma_{+} e^{i\phi_{+}} e^{i\Delta_{k}^{-} \tau}\right) + i\left(\Gamma_{-} + \gamma_{-} e^{i\phi_{-}} e^{i\Delta_{k}^{-} \tau}\right)} 10b)$$

$$t_{k-}^{+} = \frac{e^{i\phi} \frac{\pi}{v} i \left(J_{1s} + J_{2s} e^{i\Delta_{k}^{-} \tau} e^{i\phi_{+}}\right) \left(J_{1c}^{*} + J_{2c}^{*} e^{-i\Delta_{k}^{-} \tau} e^{-i\phi_{-}}\right)}{\Delta_{k}^{-} + i\left(\Gamma_{+} + \gamma_{+} e^{i\phi_{+}} e^{i\Delta_{k}^{-} \tau}\right) + i\left(\Gamma_{-} + \gamma_{-} e^{i\phi_{-}} e^{i\Delta_{k}^{-} \tau}\right)} 10c)$$

$$r_{k-}^{+} = \frac{e^{i\phi} \frac{\pi}{v} i \left(J_{1s} e^{i\Delta_{k}^{-} \tau} e^{i\phi_{+}} + J_{2s}\right) \left(J_{1c}^{*} + J_{2c}^{*} e^{-i\Delta_{k}^{-} \tau} e^{-i\phi_{-}}\right)}{\Delta_{k}^{-} + i\left(\Gamma_{+} + \gamma_{+} e^{i\phi_{+}} e^{i\Delta_{k}^{-} \tau}\right) + i\left(\Gamma_{-} + \gamma_{-} e^{i\phi_{-}} e^{i\Delta_{k}^{-} \tau}\right)} 10d)$$

where t_{k-} and r_{k-} are the amplitudes of the reflected wave and transmitted wave, t_{k-}^+ and r_{k-}^+ are the forward and backward transfer amplitudes. Phases in Eq.(10) are defined as

$$\phi_{+} = (\omega_{e} - \nu_{+}) \tau, \phi = (\nu_{+} - \nu_{-}) \tau/2 \tag{11}$$

The elastic scattering by the GA preserves the original frequency of single photons, which is described by the transmittance and reflectance, $T = |t_{k-}|^2$ and $R = |r_{k-}|^2$ respectively. The inelastic scattering changes the frequency of propagating photons by the amount $|\nu_+ - \nu_-|$, which can be adjusted by the driving field. The probability for photons with frequency conversion is described by the conversion probability $T_c = |r_{k-}^+|^2 + |t_{k-}^+|^2$. To convert frequency, $\theta \neq n\pi$ is required, i.e., the classical field must be applied. $T + R + T_c = 1$ for all frequencies indicates probability conservation for the photon. When the dissipation of the excited state to the environment except the 1D waveguide is considered, the total scattering probability is smaller than unity by reducing the scattering probabilities and increasing the linewidth of the spectra, so the dissipation of the GA is not taken into account in this paper. Since $|r_{k-}^+| \neq |t_{k-}^+|$ as long as the phase $\varphi_J \neq n\pi$, the outgoing photon displays a preferred direction, which is a consequence of breaking time-reversal symmetry. We emphasize that there is NO chiral coupling of atomic transitions to the waveguide here. The symmetry breaking should also be shown in the photon scattering process. In the 1D, its vector nature of the wave vector is reflected in the occurrence of both positive and negative values. For photons incident from different direction of the negative channel with wave vector -k < 0, the element of the scattering matrix has the same expression as Eq.(9) with -k replacing k, which leads to the following scattering amplitudes

$$\tilde{t}_{k-} = \frac{\frac{\Delta_{k}^{-} - \frac{2\pi}{v} J_{1c}^{*} J_{2c} \sin(\Delta_{k}^{-} \tau + \phi_{-}) + i\Gamma_{+} + i\gamma_{+} e^{i(\Delta_{k}^{-} \tau + \phi_{+})}}{\Delta_{k}^{-} + i\left(\Gamma_{+} + \gamma_{+} e^{i\phi_{+}} + e^{i\Delta_{k}^{-} \tau}\right) + i\left(\Gamma_{-} + \gamma_{-} e^{i\phi_{-}} e^{i\Delta_{k}^{-} \tau}\right)} 12a)$$

$$\tilde{r}_{k-} = -\frac{i\gamma_{-} + \frac{\pi}{v} i \left[|J_{1c}|^{2} e^{-i(\Delta_{k}^{-} \tau + \phi_{-})} + |J_{2c}|^{2} e^{i(\Delta_{k}^{-} \tau + \phi_{-})}}{\Delta_{k}^{-} + i\left(\Gamma_{+} + \gamma_{+} e^{i\phi_{+}} e^{i\Delta_{k}^{-} \tau}\right) + i\left(\Gamma_{-} + \gamma_{-} e^{i\phi_{-}} e^{i\Delta_{k}^{-} \tau}\right)} 12b)$$

$$\tilde{t}_{k-}^{+} = \frac{e^{-i\phi} \frac{\pi i}{v} \left[J_{1s} + J_{2s} e^{-i(\Delta_{k}^{-} \tau + \phi_{+})} \right] \left(J_{1c}^{*} + J_{2c}^{*} e^{i\Delta_{k} \tau} e^{i\phi_{-}}\right)}{\Delta_{k}^{-} + i\left(\Gamma_{+} + \gamma_{+} e^{i\phi_{+}} e^{i\Delta_{k}^{-} \tau}\right) + i\left(\Gamma_{-} + \gamma_{-} e^{i\phi_{-}} e^{i\Delta_{k}^{-} \tau}\right)} 12c)$$

$$\tilde{t}_{k-}^{+} = \frac{e^{-i\phi} \frac{\pi i}{v} \left[J_{1s} e^{-i(\Delta_{k}^{-} \tau + \phi_{+})} + J_{2s} \right] \left(J_{1c}^{*} + J_{2c}^{*} e^{i\Delta_{k} \tau} e^{i\phi_{-}}\right)}{\Delta_{k}^{-} + i\left(\Gamma_{+} + \gamma_{+} e^{i\phi_{+}} e^{i\Delta_{k}^{-} \tau}\right) + i\left(\Gamma_{-} + \gamma_{-} e^{i\phi_{-}} e^{i\Delta_{k}^{-} \tau}\right)} 12d)$$

Similarly, we define $\tilde{T}=|\tilde{t}_{k-}|^2$, $\tilde{R}=|\tilde{r}_{k-}|^2$ and $\tilde{T}_c=|\tilde{r}_{k-}^+|^2+|\tilde{t}_{k-}^+|^2$ as the transmittance, reflectance and the conversion probability for incident photons with -k, respectively. It can be found from Eqs.(11) and (12) that the reflectance $R=\tilde{R}$ and the system presents reciprocity in transmission and transfer upon reversing the propagation of an incident photon when $\varphi_J=n\pi$.

III. SINGLE-PHOTON SCATTERING SPECTRA

The scattering spectra are determined by the following parameters: the characteristic frequencies $\omega_e - \nu_{\pm}$, the delay time proportional to the distance between the

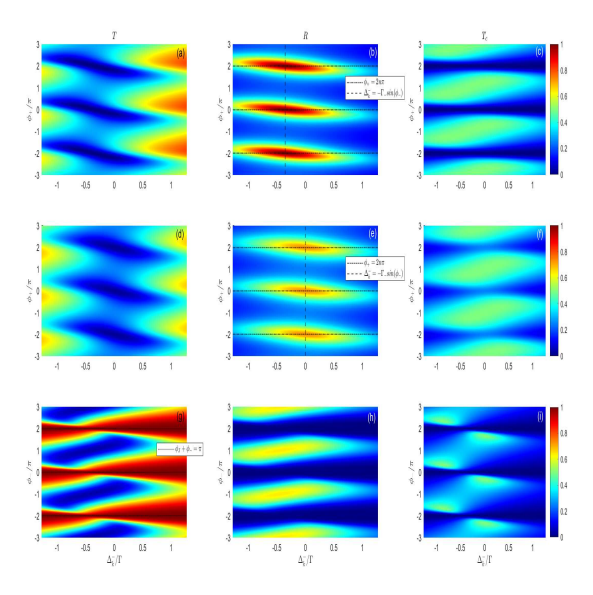


FIG. 2. (a), (d)/(g) transmittance T, (b), (e)/(h) reflectance R, and (c), and (f)/(i) conversion probability T_c versus detuning coefficient Δ_k^-/Γ and phase delay coefficient $(\phi_{+}/\pi)/(\phi_{-}/\pi)$ for (a)-(c) $\varphi_{J} = \pi, \phi_{-} = 0.75\pi$, (d)-(f) $\varphi_J = 0.75\pi, \phi_- = \pi, \text{ and (g)-(i) } \varphi_J = \pi, \phi_+ = \pi/3.$ The dashed and dash-dotted lines in (b) and (e) represent the position for maximum reflection, respectively. The dash-dotted line in (g) represents the position for total transmission. We have set $|J_1| = |J_2|$ and $\theta = \pi/2$ in all panels.

two coupling points, and the decay rate Γ . We will set $|J_1| = |J_2|$ since the system reduces to a two-level GA interaction with a 1D waveguide and total transmission can be found for a incident single photon when the driving field is absent (i.e., $\theta = 0$). In a GA-waveguide system, τ^{-1} , $\Gamma < \omega_e - \nu_{\pm}$ is usually satisfied. So we divided the discussion into two parts depending on whether τ^{-1} is comparable to or smaller than Γ .

Markovian regime

When the travel time of light between coupling points is smaller than the characteristic timescale Γ^{-1} , the factors $\exp(\pm i\Delta_k^- \tau)$ can be set to 1, but it is impossible to assume that factor $\exp(\pm i\phi_{\pm}) = 1$ since the distance is at least of the order of a resonant wavelength. Then, the scattering amplitudes for single photons incident from

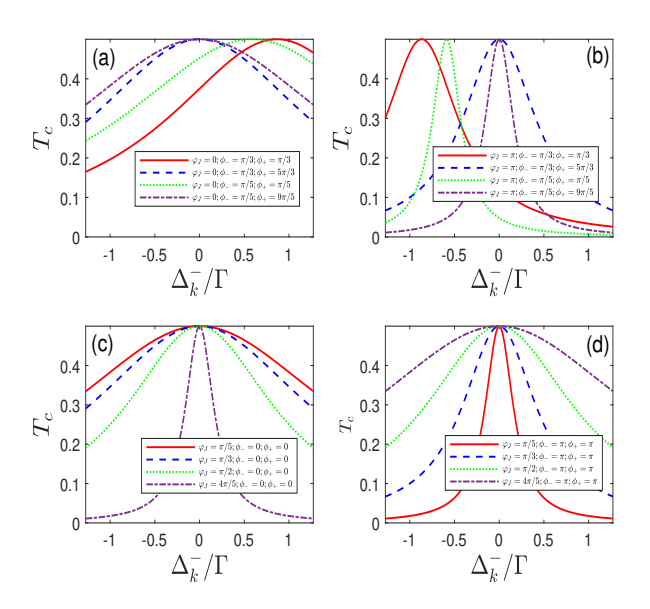


FIG. 3. The conversion probability T_c versus detuning Δ_k^-/Γ for given ϕ_{\pm}, φ_{J} . We have set $|J_{1}| = |J_{2}|$ and $\theta = \pi/2$ in all panels.

the negative channel with wave vector k > 0 reads

$$t_{k-} = \frac{\Delta_k^- - \frac{2\pi}{v} J_{1c} J_{2c}^* \sin \phi_- + i(\Gamma_+ + \gamma_+ e^{i\phi_+})}{\Delta_k^- + i(\Gamma_+ + \gamma_+ e^{i\phi_+}) + i(\Gamma_- + \gamma_- e^{i\phi_-})}$$
(13a)

$$r_{k-} = -\frac{i\gamma_{-} + \frac{\pi}{v}i(|J_{1c}|^{2}e^{i\phi_{-}} + |J_{2c}|^{2}e^{-i\phi_{-}})}{\Delta_{k}^{-} + i(\Gamma_{+} + \gamma_{+}e^{i\phi_{+}}) + i(\Gamma_{-} + \gamma_{-}e^{i\phi_{-}})}$$
(13b)

$$t_{k-}^{+} = \frac{e^{i\phi} \frac{\pi}{v} i (J_{1s} + J_{2s} e^{i\phi} +) (J_{1c}^{*} + J_{2c}^{*} e^{-i\phi} -)}{\Delta_{k}^{-} + i (\Gamma_{+} + \gamma_{+} e^{i\phi} +) + i (\Gamma_{-} + \gamma_{-} e^{i\phi} -)}$$
(13c)

$$r_{k-}^{+} = \frac{e^{i\phi} \frac{\pi}{v} i \left(J_{1s} e^{i\phi} + J_{2s}\right) \left(J_{1c}^{*} + J_{2c}^{*} e^{-i\phi}\right)}{\Delta_{k}^{-} + i \left(\Gamma_{+} + \gamma_{+} e^{i\phi}\right) + i \left(\Gamma_{-} + \gamma_{-} e^{i\phi}\right)}$$
(13d)

and the scattering amplitudes for single photons incident from the opposite direction reads

$$\tilde{t}_{k-} = \frac{\Delta_{k}^{-} - \frac{2\pi}{v} J_{1c}^{*} J_{2c} \sin \phi_{-} + i(\Gamma_{+} + \gamma_{+} e^{i\phi_{+}})}{\Delta_{k}^{-} + i(\Gamma_{+} + \gamma_{+} e^{i\phi_{+}}) + i(\Gamma_{-} + \gamma_{-} e^{i\phi_{-}})}$$
(14a)

$$\tilde{t}_{k-} = \frac{\Delta_{k}^{-} - \frac{2\pi}{v} J_{1c}^{*} J_{2c} \sin \phi_{-} + i(\Gamma_{+} + \gamma_{+} e^{i\phi_{+}})}{\Delta_{k}^{-} + i(\Gamma_{+} + \gamma_{+} e^{i\phi_{+}}) + i(\Gamma_{-} + \gamma_{-} e^{i\phi_{-}})}$$
(14a)
$$\tilde{r}_{k-} = -\frac{i\gamma_{-} + \frac{\pi}{v} i(|J_{1c}|^{2} e^{-i\phi_{-}} + |J_{2c}|^{2} e^{i\phi_{-}})}{\Delta_{k}^{-} + i(\Gamma_{+} + \gamma_{+} e^{i\phi_{+}}) + i(\Gamma_{-} + \gamma_{-} e^{i\phi_{-}})}$$
(14b)
$$\tilde{t}_{k-}^{+} = \frac{\frac{\pi i}{v} e^{-i\phi} [J_{1s} + J_{2s} e^{-i\phi_{+}}] (J_{1c}^{*} + J_{2c}^{*} e^{i\phi_{-}})}{\Delta_{k}^{-} + i(\Gamma_{+} + \gamma_{+} e^{i\phi_{+}}) + i(\Gamma_{-} + \gamma_{-} e^{i\phi_{-}})}$$
(14c)

$$\tilde{t}_{k-}^{+} = \frac{\frac{\pi \mathrm{i}}{v} e^{-\mathrm{i}\phi} \left[J_{1s} + J_{2s} e^{-\mathrm{i}\phi} + \right] \left(J_{1c}^{*} + J_{2c}^{*} e^{\mathrm{i}\phi} - \right)}{\Delta_{\nu}^{-} + \mathrm{i} \left(\Gamma_{+} + \gamma_{+} e^{\mathrm{i}\phi} + \right) + \mathrm{i} \left(\Gamma_{-} + \gamma_{-} e^{\mathrm{i}\phi} - \right)}$$
(14c)

$$\tilde{r}_{k-}^{+} = \frac{\frac{\pi i}{v} e^{-i\phi} \left[J_{1s} e^{-i\phi + J_{2s}} \right] \left(J_{1c}^{*} + J_{2c}^{*} e^{i\phi -} \right)}{\Delta_{k}^{-} + i \left(\Gamma_{+} + \gamma_{+} e^{i\phi +} \right) + i \left(\Gamma_{-} + \gamma_{-} e^{i\phi -} \right)}$$
(14d)

Reciprocal photon transmission can be found from Eqs.(13) and (14) when $\phi_{-} = n\pi$. The Markovian approximation makes the lamb shift of the excited state from a energy-dependent quantity to a energyindependent quantity.

In Fig.2, we plot the transmittance T, reflectance Rand the conversion probability T_c as functions of the scaled detuning Δ_k^-/Γ and the phase delay ϕ_+/π in the upper and middle panels, or ϕ_{-}/π in the lower panels. All scattering coefficients change periodically with

 ϕ_{\pm} . From the upper three panels (a-c), we found that when $\phi_{+} = 2n\pi$, R = 1 and T = 0 can be achieved at $\Delta_k^- = -\Gamma_- \sin \phi_-$, and photons undergo only elastic scattering since $T_c = 0$ for all incident photons with arbitrary frequencies. When we interchange the values of φ_J and φ_- , the reflectance R still achieves its maximum value at $\Delta_k^- = 0$ and $\phi_+ = 2n\pi$, but its magnitude decreases (see Fig.2e) and frequency conversion happens for photons (see Fig.2f). The lower three panels (g-i) show a frequency-independent total transmission T=1at $\phi_{-}=2n\pi$. It can be easily found from Eqs.(13) and (14) that the emission from the $|e\rangle \leftrightarrow |\eta_{+}\rangle(|\eta_{-}\rangle)$ transition is completely suppressed at $\varphi_J = (2n+1)\pi$ and $\phi_{+} = 2n\pi \ (\phi_{-} = 2n\pi)$ regardless of the value of ϕ_{-} (ϕ_+) , such suppression is caused by the formation of a GA-photon bound state. This GA-photon bound state gives rise to a photonic bound state in continuum (BIC) in the positive channel and negative channel [41, 42], respectively. Hence a total reflection R=1 can be observed as long as a BIC is formed in the positive channel, and a frequency-independent perfect transmission can be found once a BIC is formed in the negative channel. The frequency-independent $T_c = 0$ occurs when a BIC is formed in either of channels. With these underlying physics, one can found that the BIC in the positive (negative) channel also appears at $\varphi_{J} = 2n\pi$ and $\phi_{+} = (2m+1)\pi \ (\phi_{-} = (2m+1)\pi) \text{ for arbitrary } \phi_{-} \ (\phi_{+}).$ Thus, in addition to $T_c = 0$, R = 1 and T = 0 can be achieved at $\Delta_k^- = \Gamma_- \sin \phi_-$ for any $\phi_- \neq (2m+1)\pi$ when $\varphi_J = 2n\pi$ and $\phi_+ = (2n+1)\pi$, the frequencyindependent perfect transmission T = 1 occurs for arbitrary ϕ_+ when $\varphi_I = 2n\pi$ and $\phi_- = (2n+1)\pi$. To enhance the conversion probability with reciprocity presented, one has to sabotage the condition for the formation of BICs. In Fig. 3, we have plotted the T_c as a function of detuning Δ_k^-/Γ for given phases, it shows that in the presence of reciprocity, the optimal conversion probability is at most, one-half which appears at $\phi_{+} \pm \phi_{-} = 2m\pi$ for any $\phi_{-} \neq (n+1)\pi$ when $\varphi_{J} = n\pi$ or at $\phi_{+} = 2n\pi + \phi_{-} = m\pi$ for any $\varphi_{J} \neq n\pi$. The width of the conversion profile decreases gradually as φ_J increases from 0 to π when $\phi_{+} = 2n\pi + \phi_{-} = 2m\pi$ and is reversed when $\phi_{+}=2n\pi+\phi_{-}=(2m+1)\pi$, however, the position of its peak is unchanged during this process, as shown in Fig. 3(c,d). One interested condition is $\varphi_J = (n+1/2)\pi$ where the collective damping parameter γ induced by the waveguide is zero, T_c is independent of ϕ_+ (not shown here).

To increase the conversion probability further (larger than one-half), it is necessary to break the reciprocity. Eqs.(13) and (14) told us that locking either of the relations $\phi_- \pm \varphi_J = (2n+1)\pi$ could lower the reflectance sine $R = \tilde{R}$. To explore the unidirectional light transport capabilities of the system, we define the transmission contrast $I_1 = T - \tilde{T}$ and the conversion contrast $I_2 = T_c - \tilde{T}_c$. The energy conservation in the system indicates $I_1 = -I_2$. The reciprocal scattering corresponds to $I_1 = I_2 = 0$. The optimal nonreciprocal scattering

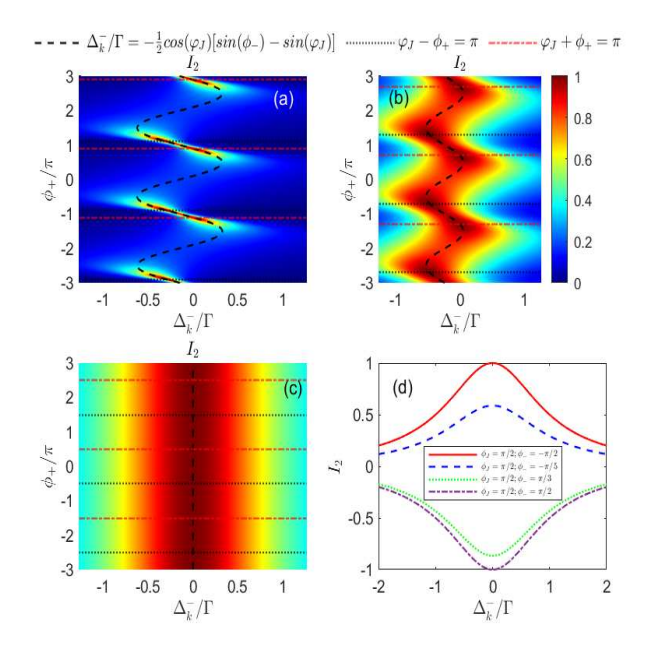


FIG. 4. The conversion contrast I_2 versus detuning Δ_k^-/Γ and ϕ_+ for (a) $\varphi_J=0.1\pi, \phi_-=1.1\pi$, (b) $\varphi_J=0.3\pi, \phi_-=1.3\pi$, (c) $\varphi_J=0.5\pi, \phi_-=1.5\pi$. (d) The conversion contrast for different ϕ_- when $\varphi_J=\pi/2$. We have set $|J_1|=|J_2|$ and $\theta=\pi/2$.

yields $|I_1| = |I_2| = 1$, then the efficiency of the frequency conversion approaches unity since the scattering coefficients can not be smaller than zero. We have plotted the conversion contrast I_2 versus the scaled detuning Δ_k^-/Γ and phase delay ϕ_+ with $\phi_- - \varphi_J = \pi$ in Fig. 4(a-c). Fig. 4(a) and (b) show that I_2 can reaches maximum at $\Delta_k^- = \gamma_+ \sin \phi_+ + \gamma_- \sin \phi_-$, its optimal conversion probability is one, which occurs at two positions (see the cross between the dashed line and the red dotted-dash line for $\phi_+ + \varphi_J = \pi$ as well as the cross between the dashed line and the dotted line for $\phi_+ - \varphi_J = \pi$). One is located at $\Delta_k^- = 0$, i.e., the incident photon is on resonance with the $|e\rangle \leftrightarrow |\eta_{-}\rangle$ transition, the reason for the appearance of $\Delta_k^- = 0$ is that the lamb shift induced by the two channels cancels out each other due to $\phi_{+} + \phi_{-} = 2n\pi$. However, the lamb shift presents at the condition $\phi_+ - \phi_- = 2n\pi$, which results in the other position of the optimum. Fig. 4(c) shows that the unity of the conversion contrast always occurs at $\Delta_k^- = 0$, and it is independent of phase delay ϕ_+ when $\varphi_J = (n + 0.5)\pi$, i.e., it is only a function of Δ_k^- . So we plot Fig. 4(d) to present how the optimal I_2 depends on the phase ϕ_- at $\varphi_J = \pi/2$. It shows that the phase delay ϕ_- controls the optimal value of I_2 when the waveguide-mediated nonlocal damping $\gamma = 0$.

B. Non-Markovian regime

When the travel time of light between coupling points is comparable to the characteristic timescale Γ^{-1} , the

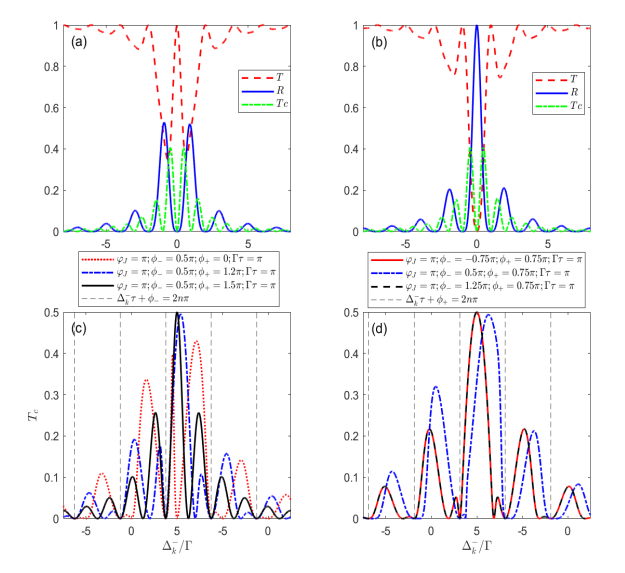


FIG. 5. (a, b)The transmittance $T=\tilde{T}$ (dashed red curve), reflectance $R=\tilde{R}$ (solid blue curve) and the conversion probability $T_c=\tilde{T}_c$ (dotted-dash green curve) versus detuning Δ_k^-/Γ when $\varphi_J=(2n+1)\pi$, (a) $\tau\Gamma=1.0025\pi$ and (b) $\tau\Gamma=0.9975\pi$. We have set $|J_1|=|J_2|,~\theta=\pi/2,~\omega_e=600\Gamma,~\Omega=1.5\Gamma$. (c, d) The conversion probability T_c versus detuning Δ_k^- for given ϕ_{\mp} and $\varphi_J=(2n+1)\pi$.

factors $\exp(\pm i\Delta_k^- \tau)$ varies with detuning Δ_k^- , so it is impossible to keep the reflectance zero by locking the relation of the phases or to observe the frequencyindependent perfect transmission. In Fig. 5(a,b), we have plotted the transmittance, the reflectance and the conversion probability as a function of the scaled detuning Δ_k^-/Γ when $\varphi_J = n\pi$. The spectra in Fig. 5(a,b) show multiple peaks and dips, and the number of peaks and dips increase with τ increases. The emission from the $|e\rangle \leftrightarrow |\eta_{-}\rangle$ transition is completely suppressed when $\Delta_k^- \tau + \phi_- = 2m\pi$ with $\varphi_J = (2n+1)\pi$, so the peaks of the transmittance reach unity, and the reflectance and conversion probability vanish correspondingly. The condition $\Delta_k^- \tau + \phi_+ = 2m\pi$ with $\varphi_J = (2n+1)\pi$ leads to the suppression of emission from the $|e\rangle \leftrightarrow |\eta_{+}\rangle$ transition, so the conversion probability takes the value of zero. Although there are many peaks of reflectance, the total reflectance requires the real part of the denominator in Eqs.(11) and (12) to be zero and the suppression of the emission from the $|e\rangle \leftrightarrow |\eta_{+}\rangle$ transition. Note that the positions where the peaks of the reflectance located do not correspond to those of the conversion dips. In Fig. 5(c,d), we plot T_c versus detuning for given ϕ_{\pm} and $\varphi_J = (2n+1)\pi$. The conversion dips can be divided into two categories: one is static, while the other moves with the phase ϕ_+ in Fig. 5c (ϕ_- in Fig. 5d). The static dips satisfy $\Delta_k^- \tau + \phi_- = 2m\pi$ in Fig. 5c $(\Delta_k^- \tau + \phi_+) = 2n\pi$ in Fig. 5d), the moving dips satisfy $\Delta_k^- \tau + \phi_+ = 2n\pi$

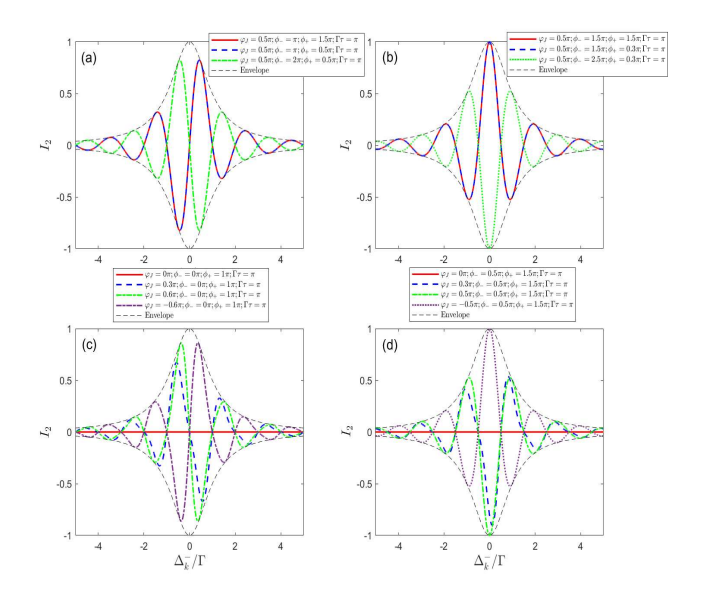


FIG. 6. The conversion contrast I_2 versus detuning Δ_k^-/Γ when $\Gamma \tau = \pi$. (a,b) $\varphi_J = 0.5\pi$, (c) $\phi_- = 0, \phi_+ = \pi$ (d) $\phi_- = 0.5\pi, \phi_+ = 1.5\pi$.

in Fig. 5c ($\Delta_k^-\tau + \phi_- = 2n\pi$ in Fig. 5d), it indicates that the dips of T_c arise from the suppression of emission in either positive channel or negative channel. Thence, one can control the positions of the conversion dips flexibly by tuning the phases ϕ_\pm . Fig. 5(c,d) show that the conversion probability is symmetric to $\Delta_k^- = 0$ when $\phi_+ + \phi_- = 2n\pi$, see the black solid line in Fig. 5(c) as well as the black dashed line and the red solid line in Fig. 5(d); the optimal conversion probability is at most one-half since photon scattering coefficients are symmetric for the forward and backward propagation directions. Thus as long as the system is reciprocal, one-half is the upper bound of the conversion probability.

The previous discussion demonstrates that preventing the suppression of the GA's emission is the first step to improving conversion probability, and breaking the reciprocity is the second step to further enhance the conversion probability. When $\varphi_J = \pi/2$, the nonlocal damping γ is absent, the GA in the excited state decays into states $|\eta_{-}\rangle$ and $|\eta_{+}\rangle$ at the same rate, and the Lamb shift induced by the vacuum disappears. Fig. 6(a,b) depicts the conversion contrast I_2 versus the detuning when $\Gamma \tau = \pi$. Similar to I_2 in the Markovian regime, the conversion contrast I_2 is also independent of phase delay ϕ_+ (see the red solid line and the blue dashed line in Fig. 6(a,b)), and phase delay ϕ_{-} controls its optimal value. We also found that the decay rate of the GA to both channels are equal and the Lamb shift is absent when $\phi_+ - \phi_- = (2n+1)\pi$, I_2 in this case is also plotted in Fig. 6(c,d) for fixed ϕ_{\pm} and different φ_J . The graphs of Fig. 6 exhibit oscillatory behaviors, and the peaks and dips of these oscillations form stable envelopes. Graphs in Fig. 6(a,c) are symmetric about the point $\Delta_k = 0$, i.e., I_2 is an odd function

of Δ_k . Though one can improve I_2 closer to one by increasing τ , the conversion contrast of one is unattainable. Graphs in Fig. 6(b,d) are symmetric about the $\Delta_k^- = 0$ axis, i.e., I_2 is an even function of Δ_k , thus the conversion contrast reaches ± 1 . The conversion probability $T_c = 1$ when $I_2 = 1$. Besides the vanishing of the reflectance, the waves emitted by the GA and propagated along the forward direction in the waveguide interference destructively for photon incident from the forward direction, however, the waves emitted by the GA and propagated along the backward direction in the waveguide interference constructively for photon incident from the backward direction. In addition, Fig. 6(c,d) show that the optimal nonreciprocal scattering only achieves at $\varphi_J = (n+0.5)\pi$.

IV. CONCLUSION

We consider a V-type GA, where the field in a conventional waveguide with linear light dispersion and the driving field interact with the GA on the transitions $|g\rangle \leftrightarrow |e\rangle$ and $|g\rangle \leftrightarrow |f\rangle$, correspondingly. Single photons traveling in the waveguide can be scattered by the GA elastically and inelastically at two coupling points. The inelastic scattering realizes the single-photon frequency conversion as the GA spontaneously decays to a superposition state of $|q\rangle$ and $|f\rangle$ orthogonal to its initial state. The scattering coefficients for photons incident from forward and backward directions are obtained via the Lippmann-Schwinger equation, which display quite different scattering spectra in the Markovian and Non-Markovian regimes which is defined according to the relative relation of the travel time of the photon between the coupling points and the inverse of the bare relaxation rate of the GA. We have studied the influence of the accumulated phases ϕ_{\pm} that photons travel between coupling points and the phase difference φ_i between the two coupling strengths on the scattering spectra as well as

the conversion contrast which characterize nonreciprocal single-photon scattering in both regimes. Light transport is symmetric for the forward and backward propagation direction at $\varphi_i = n\pi$ in both regimes, the optimal conversion probability is at most, one-half, and it can surpass the limit one-half and reach unity by breaking the reciprocity. In the Markovian regime, in addition to the reciprocal behavior of single photons at $\phi_{-} = n\pi$, the formation of the photonic BIC in the elastic scattering process gives rise to the frequency-independent total transmission, and the BIC in inelastic scattering process generates the total reflection. In the non-Markovian regime, the spectra and the contrast show multiple peaks and dips, and the number of peaks and dips increase as the scale of a two-legged giant atom increases. Total transmissions occurs only for the single-photon with frequency which can suppress the emission from the GA's transition to its initial state. More stringent conditions are required to achieve the total reflection. The suppression of the emission from either transitions results in the conversion probability vanishing. When the GA in the excited state decays into its initial state and the superposition state orthogonal to its initial state at the same rate, the conversion contrast exhibits the oscillatory behaviors, the peaks and dips of these oscillations form stable envelopes, and the conversion contrast can be an odd or even function of the detuning. Although single-photon frequency up- or down-conversion with efficiency close to unity can be achieved by increasing the scale of the GA, its optimal unity occurs only when the incident photon is on resonance with the GA.

ACKNOWLEDGMENTS

This work was supported by NSFC Grants No.12247105, No.12421005, XJ-Lab Key Project (23XJ02001), and the Science & Technology Department of Hunan Provincial Program (2023ZJ1010).

- K. M. Birnbaum, A. Boca, R. Miller, A. D. Boozer, T. E. Northup, and H. J. Kimble, Photon Blockade in an Optical Cavity with One Trapped Atom, Nature (London) 436, 87 (2005).
- [2] C. Hamsen, K. N. Tolazzi, T. Wilk, and G. Rempe, Two-Photon Blockade in an Atom-Driven Cavity QED System, Phys. Rev. Lett. 118, 133604 (2017).
- [3] A. Reinhard, T. Volz, M. Winger, A. Badolato, K.J. Hennessy, E. L. Hu, and A. Imamoğlu, Strongly Correlated Photons on a Chip, Nat. Photonics 6, 93 (2012).
- [4] A. Javadi, I. Söllner, M. Arcari, S. L. Hansen, L. Midolo, S. Mahmoodian, G. Kiršanskė, T. Pregnolato, E. H. Lee, J. D. Song, S. Stobbe, and P. Lodahl, Single-Photon Non-Linear Optics with a Quantum Dot in a Waveguide, Nat. Commun. 6, 8655 (2015).
- [5] P. Bermel, A. Rodriguez, S. G. Johnson, J. D. Joannopoulos, and M. Soljačić, Single-photon all-optical

- switching using waveguide-cavity quantum electrodynamics, Phys. Rev. A 74, 043818 (2006).
- [6] L. Zhou, Z. R. Gong, Y.-X. Liu, C. P. Sun, and F. Nori, Controllable Scattering of a Single Photon inside a One-Dimensional Resonator Waveguide, Phys. Rev. Lett. 101, 100501 (2008).
- [7] D. Aghamalyan, J.-B. You, H.-S. Chu, C. E. Png, L. Krivitsky, and L. C. Kwek, Tunable quantum switch realized with a single Λ-level atom coupled to the microtoroidal cavity, Phys. Rev. A 100, 053851 (2019).
- [8] E. V. Stolyarov, Single-photon switch controlled by a qubit embedded in an engineered electromagnetic environment, Phys. Rev. A 102, 063709 (2020).
- [9] Mateusz Duda, Luke Brunswick, Luke R. Wilson, and Pieter Kok, Efficient, high-fidelity single-photon switch based on waveguide-coupled cavities, Phys. Rev. A 110 042615 (2024)

- [10] I. C. Hoi, C. M. Wilson, G. Johansson, T. Palomaki, B. Peropadre, and P. Delsing, Demonstration of a Single-Photon Router in the Microwave Regime, Phys. Rev. Lett. 107, 073601 (2011).
- [11] L. Zhou, L. P. Yang, Y. Li, and C. P. Sun, Quantum Routing of Single Photons with a Cyclic Three-Level System Phys. Rev. Lett. 111, 103604 (2013).
- [12] J. Lu, L. Zhou, L. M. Kuang, and F. Nori, Single-photon router: Coherent control of multichannel scattering for single photons with quantum interferences, Phys. Rev. A 89, 013805 (2014).
- [13] J. Lu, Z. H. Wang, and L. Zhou, T-shaped single-photon router, Opt. Exp. 23, 22955 (2015).
- [14] D. C. Yang, M. T. Cheng, X. S. Ma, J. P. Xu, C. J. Zhu, and X. S. Huang, Phase-modulated single-photon router, Phys. Rev. A 98, 063809 (2018).
- [15] Y. L. Ren, S. L. Ma, J. K. Xie, M. T. Cao, and F. L. Li, Nonreciprocal single-photon quantum router, Phys. Rev. A 105, 013711 (2022).
- [16] C. Gonzalez-Ballestero, E. Moreno, F. J. Garcia-Vidal, and A. Gonzalez-Tudela, Nonreciprocal few-photon routing schemes based on chiral waveguide-emitter couplings, Phys. Rev. A 94, 063817 (2016).
- [17] C. H. Yan, Y. Li, H. D. Yuan, and L. F. Wei, Targeted photonic routers with chiral photon-atom interactions, Phys. Rev. A 97, 023821 (2018).
- [18] M. Ahumada, P. A. Orellana, F. Domíguez-Adame, and A. V. Malyshev, Tunable single-photon quantum router, Phys. Rev. A 99, 033827 (2019).
- [19] Z. Wang, Y. Wu, Z. Bao, Y. Li, C. Ma, H. Wang, Y. Song, H. Zhang, and L. Duan, Experimental realization of a deterministic quantum router with superconducting quantum circuits, Phys. Rev. Appl. 15, 014049 (2021).
- [20] D. Roy, Few-photon optical diode, Phys. Rev. B 81, 155117 (2010).
- [21] W.-B. Yan, W.-Y. Ni, J. Zhang, F.-Y. Zhang, and H. Fan, Tunable single-photon diode by chiral quantum physics, Phys. Rev. A 98, 043852 (2018).
- [22] J. L. Tan, X. W. Xu, J. Lu, and L. Zhou, Few-photon optical diode in a chiral waveguide, Opt. Express 30, 28696 (2022).
- [23] M. V. Gustafsson, T. Aref, A. F. Kockum, M. K. Ekström, G. Johansson, and P. Delsing, Propagating phonons coupled to an artificial atom, Science 346, 207 (2014).
- [24] R. Manenti, A. F. Kockum, A. Patterson, T. Behrle, J. Rahamim, G. Tancredi, F. Nori, and P. J. Leek, Circut quantum acoustodynamics with surface acoustic waves, Nat. Commun. 8, 975 (2017). (2017).
- [25] G. Andersson, M. K. Ekström, and P. Delsing, Electromagnetically Induced Acoustic Transparency with a Superconducting CircuitPhys. Rev. Lett. 124, 240402 (2020).
- [26] A. M. Vadiraj, A. Ask, T. G. McConkey, I. Nsanzineza, C. W. Sandbo Chang, A. F. Kockum, and C. M. Wilson, Engineering the level structure of a giant artificial atom in waveguide quantum electrodynamics, Phys. Rev. A 103, 023710 (2021).
- [27] B. Kannan, M. J. Ruckriegel, D. L. Campbell, A. Frisk Kockum, J. Braumüller, D. K. Kim, M. Kjaergaard, P. Krantz, A. Melville, B. M. Niedzielski et al., Nature (London) 583, 775 (2020).
- [28] A. M. Vadiraj, A. Ask, T. G. McConkey, I. Nsanzineza, C.W. S.Chang, A. F. Kockum, and C. M. Wilson, Phys.

- Rev. A 103, 023710 (2021).
- [29] A. Frisk Kockum, P. Delsing, and G. Johansson, Designing frequency-dependent relaxation rates and Lamb shifts for a giant artificial atom, Phys. Rev. A 90, 013837 (2014).
- [30] G. Andersson, B. Suri, L. Guo, T. Aref, and P. Delsing, Non-exponential decay of a giant artificial atom, Nat. Phys. 15, 1123 (2019).
- [31] S. Longhi, Photonic simulation of giant atom decay, Opt. Lett. 45, 3017 (2020).
- [32] H. Pichler and Pe. Zoller, Photonic Circuits with Time Delays and Quantum Feedback, Phys. Rev. Lett. 116, 093601 (2016).
- [33] F. Roccati, and D. Cilluffo, Controlling Markovianity with Chiral Giant Atoms, Phys. Rev. Lett. 133, 063603 (2024).
- [34] L. Z. Guo, A. F. Kockum, F. Marquardt, and G. Johansson, Oscillating bound states for a giant atom, Phys. Rev. Res. 2, 043014 (2020).
- [35] X. Wang, T. Liu, A. F. Kockum, H.-R. Li, and F. Nori, Tunable chiral bound states with giant atoms, Phys. Rev. Lett. 126, 043602 (2021).
- [36] K. H. Lim, W.-K. Mok, and L.-C. Kwek, Oscillating bound states in non-Markovian photonic lattices, Phys. Rev. A 107, 023716 (2023).
- [37] X.J. Zhang, C.G. Liu, Z.R. Gong, and Z.H. Wang, Quantum interference and controllable magic cavity QED via a giant atom in a coupled resonator waveguide, Phys. Rev. A, 108, 013704 (2023).
- [38] Z. Y. Li and H. Z. Shen, Non-Markovian dynamics with a giant atom coupled to a semi-infinite photonic waveguide, Phys. Rev. A 109, 023712 (2024).
- [39] Y. Y. Yan and Z. G. Lv, Controllable spontaneous emission spectrum in an artificial giant atom: Dark lines and bound states, Phys. Rev. Res. 6, 013301 (2024).
- [40] D.-W. Wang, C. S. Zhao, Y.-T. Yan, J. Y. Yang, Z. H. Wang, and L. Zhou, Topology-dependent giant-atom interaction in a topological waveguide QED system, Phys. Rev. A 109, 053720 (2024).
- [41] Y. Yang, G. Sun, J. Li, J. Lu, and L. Zhou, Coherent Control of Spontaneous Emission for a giant driven Λtype three-level atom, Phys. Rev. A, 111, 013707 (2025)
- [42] G. Sun, Y. Yang, J. Li, J. Lu, and L. Zhou, Cavity-modified oscillating bound states with a Λ-type giant emitter in a linear waveguide, Phys. Rev. A, 111, 033701 (2025).
- [43] A. C. Santos and R. Bachelard, Generation of Maximally Entangled Long-Lived States with Giant Atoms in a Waveguide, Phys. Rev. Lett. 130, 053601 (2023).
- [44] A. F. Kockum, G. Johansson, and F. Nori, Decoherence-Free Interaction between Giant Atoms in Waveguide Quantum Electrodynamics, Phys. Rev. Lett. 120, 140404 (2018).
- [45] A. Soro and A. F. Kockum, Chiral quantum optics with giant atoms, Phys. Rev. A 105, 023712 (2022).
- [46] W.J. Gu, L. Chen, Z. Yi, S.J. Liu, and G.-X. Li, Tunable photon-photon correlations in waveguide QED systems with giant atoms, Phys. Rev. A 109 023720 (2024).
- [47] M.Z. Weng, H.W. Yu, and Z.H. Wang, High-fidelity generation of Bell and W states in a giant-atom system via bound states in the continuum, Phys. Rev. A 111 053711 (2025).
- [48] X.-L. Yin, H.-W. Joseph Lee, and G.F. Zhang, Giantatom dephasing dynamics and entanglement generation

- in a squeezed vacuum reservoir, Phys. Rev. A 111 033707 (2025).
- [49] L. Du, M. R. Cai, J. H. Wu, Z. H. Wang, and Y. Li, Single photon nonreciprocal excitation transfer with non-Markovian retarded effects, Phys. Rev. A 103, 053701 (2021).
- [50] H.W. Yu, Z.H. Wang, and J.-H. Wu, Entanglement preparation and nonreciprocal excitation evolution in giant atoms by controllable dissipation and coupling, Phys. Rev. A 104, 013720 (2021).
- [51] M. Bradford, K. C. Obi, and J.-T. Shen, Efficient Single-Photon Frequency Conversion Using a Sagnac Interferometer, Phys. Rev. Lett. 108, 103902 (2012); M. Bradford, J.-T. Shen, Single-photon frequency conversion by exploiting quantum interference, Phys. Rev. A 85, 043814 (2012).
- [52] Z. H. Wang, Lan Zhou, Yong Li, and C. P. Sun, Controllable single-photon frequency converter via a one-dimensional waveguide, Phys. Rev. A 89, 053813 (2014)
- [53] W. Z. Jia, Y. W. Wang, and Y.-X. Liu, Efficient singlephoton frequency conversion in the microwave domain using superconducting quantum circuits, Phys. Rev. A 96, 053832 (2017)
- [54] L. Du and Y. Li, Single-photon frequency conversion via a giant Λ-type atom, Phys. Rev. A 104, 023712 (2021).
- [55] L. Du, Y.-T. Chen, and Y. Li, Nonreciprocal frequency conversion with chiral Λ -type atoms, Phys. Rev. Res 3, 043226 (2021)
- [56] J. R. Taylor, Scattering Theory: The Quantum Theory on Nonrelativistic Collisions (Wiley, New York, 1972).